Shadows and Mirrors: Reconstructing Quantum States of Atom Motion

Quantum mechanics allows us only one incomplete glimpse of a wavefunction, but if systems can be identically prepared over and over, quantum equivalents of shadows and mirrors can provide the full picture.

Dietrich Leibfried, Tilman Pfau and Christopher Monroe

Imagine that a pair of coins are tossed in a black box. The box reports only one of the following three results at random: (1) the outcome of the first coin (heads or tails), (2) the outcome of the second coin (heads or tails), or (3) whether the outcomes of the two coins matched or were different. Our task is to construct a joint probability distribution of the four possible outcomes of the coins (HH, TT, HT, TH) based on many observations of the black box outputs. Now suppose that after many trials, the black box reports that each coin comes up heads two-thirds of the time when measured individually, yet the coins *never* match when they are compared. (Clearly the results of the coin tosses have been correlated—perhaps a joker in the black box flips the coins and then changes the outcomes appropriately.) We seek a distribution that both reflects this correlation and obeys the marginal distributions of each coin as two-thirds heads, one-third tails (see the three tables on page 23). The only way to satisfy both requirements is to force the joint probability $P(\mathrm{TT})$ of getting two tails to be negative! Mathematically, this is because $P(\mathrm{HH}) + P(\mathrm{TT})$ is observed to be zero, yet we expect $P(\mathrm{HH})$ to be greater than $P(\mathrm{TT})$, because the individual coins are weighted toward heads.

The sleight of hand giving rise to negative probabilities is that we have attempted to reconstruct a joint probability distribution without ever having observed individual joint outcomes of the coins. The only measured events are described by sums of joint probabilities such as $P(\mathrm{HT}) + P(\mathrm{TH}) = 1$ or $P(\mathrm{HH}) + P(\mathrm{HT}) = \frac{2}{3}$. One way to interpret the distribution of table 3 is to note that, since individual joint outcomes of the coins are inaccessible, nothing prevents us from assigning negative probabilities to such immeasurable events. With this rule in mind, this joint "quasi-probability" distribution may be a useful bookkeeping tool, as it not only characterizes the hidden correlations within the black box, but also retains information about the marginal probabilities of the individual coins.[1]

Although this example of coins in a black box is highly artificial, a similar situation arises in nature when we describe the probability distribution of a quantum mechanical particle in position–momentum phase space. A classical particle occupies a single point in phase space, and an ensemble of classical particles can be characterized by a phase-space probability distribution. On the other hand, the Heisenberg uncertainty relationship requires that a quantum mechanical particle be described by an area of uncertainty in phase space no smaller than $\Delta x\,\Delta p = \hbar/2$. If a particle's position is known well, then its momentum is not, and vice versa. In mathematical language, the position wavefunction $\Psi_x(x)$ and momentum wavefunction $\Psi_p(p)$ are related by a Fourier transform; thus, localized position wavefunctions lead to delocalized momentum wavefunctions, and vice versa. A probability distribution in quantum phase space must somehow incorporate this feature.

Wigner distribution and 'negative probabilities'

In 1932, Eugene Wigner presented a convenient mathematical construct for visualizing quantum trajectories in phase space.[2] The Wigner distribution, or Wigner function $W(x, p)$, retains many of the features of a probability distribution, except that it can be negative in some regions of phase space. In the coin example above, practical use of the quasi-probability distribution of table 3 is limited to events described by sums of any two entries. Similarly, when we apply the Wigner distribution to measurements in quantum phase space, the probability distribution for the outcome of a measurement is obtained essentially by convolving $W(x, p)$ with a distribution of possible states of the measurement device, which must be distributed over an area of order $\hbar$ or larger. This prescription leads to a natural connection between quantum and classical phase space: As the measurement resolution is degraded away from the quantum limit so that the Heisenberg uncertainty relationship plays no role, localized regions of $W(x, p)$ (with possible negative values) become washed out, and the convolved Wigner distribution approaches the usual classical phase-space probability distribution. Similar to the quasi-distribution of the coins above, the Wigner distribution is not a *bona fide* probability distribution, but can be a useful bookkeeping tool that high-

DIETRICH LEIBFRIED *is a physicist at Innsbruck University in Austria. He was a guest researcher at the National Institute of Standards of Technology in Boulder, Colorado, during the writing of this article.* TILMAN PFAU *is a physicist at the University of Konstanz in Germany.* CHRISTOPHER MONROE *is a staff physicist at the National Institute of Standards and Technology in Boulder, Colorado.*

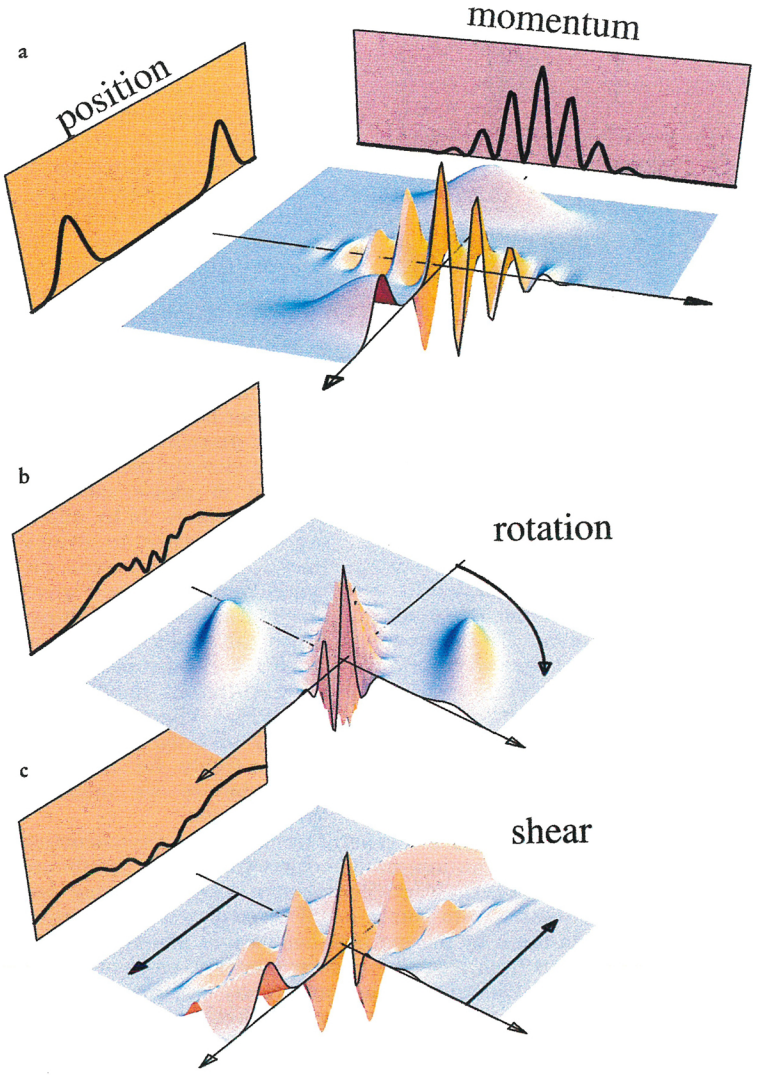

FIGURE 1: WIGNER FUNCTION FOR THE DOUBLE-SLIT EXPERIMENT, visualized in phase space. **a:** The initial Wigner distribution representing the superposition of two Gaussian lobes directly behind the slits. The oscillating part in the center is due to the spatial coherence between the two lobes. The "spacelike shadow" (on the orange screen, at left) shows the spatial marginal distribution $|\Psi_x(x)|^2$ of the state, obtained by ignoring the momentum information. The pale burgundy shadow at rear shows the corresponding "momentum-like shadow" $|\Psi_p(p)|^2$. With a position-sensitive detector measuring the spacelike shadow, we can view the initial Wigner distribution from different angles by either rotating it (**b**) or shearing it (**c**).

lights the inherent anticorrelation of position and momentum uncertainty.

For a pure quantum state, the Wigner distribution is related to the position or momentum wavefunction by

$$W(x,p) = \frac{1}{2\pi}\int_{-\infty}^{\infty} \Psi_x^*\left(x-\frac{s}{2}\right)\Psi_x\left(x+\frac{s}{2}\right)e^{-isp}\,ds$$

$$= \frac{1}{2\pi}\int_{-\infty}^{\infty} \Psi_p^*\left(p+\frac{s}{2}\right)\Psi_p\left(p-\frac{s}{2}\right)e^{-isx}\,ds\,, \qquad (1)$$

where we have set $\hbar = 1$. The Wigner distribution of a mixed quantum state is a weighted sum of either expression over the appropriate wavefunctions. These expressions may not be very illuminating, and the equivalent of the Schrödinger equation describing the time evolution of $W(x,p)$ is even less so. (However, Wolfgang Schleich and Georg Süssmann discussed a physical interpretation of this form of the Wigner distribution in PHYSICS TODAY, October 1991, page 146.) Nevertheless, Wigner showed that $W(x,p)$ is indeed the closest thing we have to a probability distribution in quantum phase space, as it corresponds to the phase-space probability distribution in the classical

TABLES: **Joint probability distributions of the outcomes of tossing two coins.** (1) Probability distribution given that the two coins are tossed independently, both weighted toward heads with $P(\text{H}) = \frac{2}{3}$ and $P(\text{T}) = \frac{1}{3}$. The marginal probabilities of the outcomes of either coin (obtained by adding the entries vertically or horizontally) result in two-thirds heads and one-third tails. (2) Probability distribution given that the coins are tossed in a black box that reports that the coins never match—that is, $P(\text{HH}) + P(\text{TT}) = 0$. The off-diagonals add to 1 as required, with p arbitrary. The marginal probabilities can no longer be two-thirds heads for both coins. (3) "Quasi-probability" distribution under same conditions as (2) and also exhibiting marginal probabilities of each coin as two-thirds heads and one-third tails. The price paid is that one of the entries is negative!

(1)

	H	T
H	4/9	2/9
T	2/9	1/9

(2)

	H	T
H	0	p
T	$1-p$	0

(3)

	H	T
H	1/6	1/2
T	1/2	−1/6

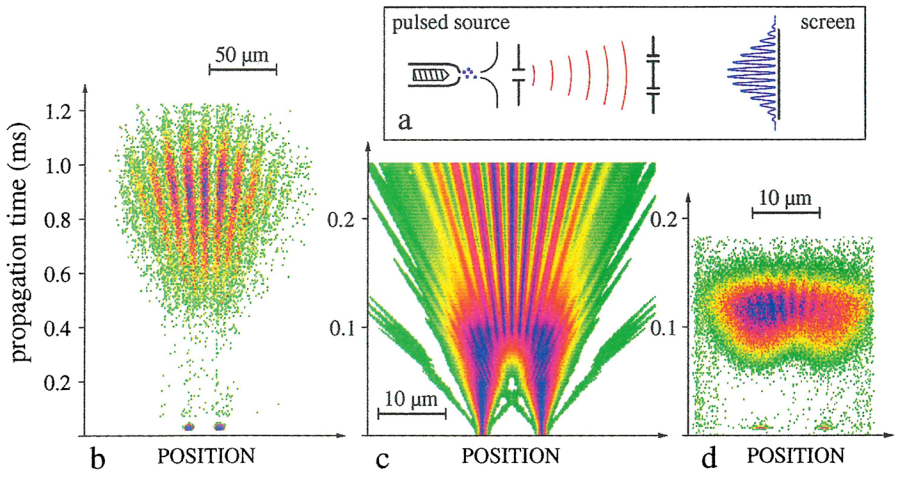

FIGURE 2: DOUBLE-SLIT ATOM INTERFEROMETRY. **a:** The experimental arrangement. Atoms from a collimated source propagate through a double slit with 8 μm separation and strike a position-sensitive detector screen. The source produces fast-moving atoms and a range of slower atoms. **b:** Diffraction pattern of the atomic matter waves plotted as a function of position and of the propagation time t_d for the atoms to travel from the double slit to the detector. The distance from double slit to detector is d = 195 cm, for which the slow atoms propagate long enough to produce a Fraunhofer (far-field) diffraction pattern. The fast atoms produce the near-field shadow of the slits at the bottom. (This shadow is magnified because of the geometry of the apparatus.) **c:** Calculated diffraction pattern for atoms having a wide range of velocities (and propagation times t_d), showing the transition between Fresnel (near-field) and Fraunhofer diffraction. **d:** Data for d = 25 cm, where the transition between Fresnel and Fraunhofer diffraction becomes visible in the slow atoms' pattern.

limit, and also preserves the marginal probability distributions of position and momentum $|\Psi_x(x)|^2$ and $|\Psi_p(p)|^2$:

$$|\Psi_x(x)|^2 = \int_{-\infty}^{\infty} W(x,p)\,dp \quad \text{and} \quad |\Psi_p(p)|^2 = \int_{-\infty}^{\infty} W(x,p)\,dx\,. \quad (2)$$

Can the Wigner distribution $W(x,p)$ of a quantum particle be measured? At first glance, the answer appears to be no. The probability distribution of any physical observable corresponds to an integral over $W(x,p)$, as in equation 2, so a single measurement cannot provide localized values of $W(x,p)$. But if we prepare a particle in the same quantum state in repeated experiments, we can perform a large number of measurements on effectively the same quantum system. We can then reconstruct the Wigner distribution by measuring various shadows or projection integrals of $W(x,p)$ in separate experiments, or by averaging an observable whose expectation value is proportional to $W(x,p)$ in repeated experiments.[3]

In the following, we describe two methods for reconstructing the Wigner distribution of atomic motion in phase space from such a set of repeated measurements. In one experiment, identically prepared atoms from a beam travel through a double-slit interferometer, and different measurements are performed on them. In another experiment, a single trapped atom is repeatedly prepared in an identical state of motion, and a different measurement is performed after each preparation. The atoms in both experiments are prepared in nonclassical states of phase space; thus their corresponding Wigner distributions have features not found in classical phase-space distributions, such as negative values.

Quantum shadows and the double slit

Detecting the positions of many identically prepared atoms yields the spatial marginal distribution $|\Psi_x(x)|^2$ as a "spacelike shadow" of the Wigner distribution; likewise, a momentum-sensitive detector yields the "momentum-like shadow" $|\Psi_p(p)|^2$. As shown in figure 1a, we can observe shadows across different angles in phase space either by rotating the detector's point of view or by rotating the Wigner distribution and keeping the detector fixed. For example, figure 1b shows the Wigner distribution rotated by 60° and measured with a position detector. The spacelike shadow on the screen now contains information about both x and p of the initial distribution. The Wigner distribution can be sheared in phase space as shown in figure 1c by allowing the particle to evolve freely. A shear rotates the spacelike shadow and gives an additional stretching, which can easily be compensated for. Thus, we can observe different shadows of the initial Wigner distribution by allowing particles to evolve freely for different times before we measure their position.

Tomography is a general technique for reconstructing the shape of an inaccessible object from a set of different shadows of that object. For instance, medical imaging uses this technique to obtain a full three-dimensional picture of the brain by piecing together various two-dimensional shadows from x rays or nuclear magnetic resonance techniques. Quantum state tomography has been used to reconstruct the quantum state of light waves[4] and molecular vibration,[5] and has also been theoretically considered for the reconstruction of the Wigner distribution of atoms from an atomic beam.[6] All these applications use a mathematical device called the inverse Radon transformation to generate an image of the higher dimensional object from a full set of shadows. In this sense, quantum mechanics places the observer in the situation of Plato's prisoner—chained in a cave so he can see only the shadows of objects outside the cave, not the objects themselves. However, when the objects are rotated or sheared, even Plato's prisoner can obtain a full picture of the objects.

At the University of Konstanz, Jürgen Mlynek's group use this tomographic technique in sending an atomic beam through a double-slit apparatus and reconstructing the Wigner distribution of the atoms immediately behind the slit.[7] The theoretical Wigner distribution in figure 1a depicts the idealized quantum state of the transverse position and momentum of each atom as it leaves the double slit. For a plane matter wave, the emerging quantum state is a linear superposition of one atomic wavepacket going through one slit and another such packet going through the other. The coherence between these two wavepackets leads to an interference pattern in the momentum distribution. The signature of this coherence in the Wigner distribution is the oscillating positive and negative values between the two main lobes. In the experiment, the spatial distribution of the atoms is measured on a screen. As the atoms freely propagate between the double slit and the screen, the corresponding quantum

state is sheared in phase space as shown in figure 1c. Different atoms experience different shear, since they are distributed over a broad range of velocities and therefore evolve for different times as they travel from the double slit to the detector. A velocity-selective experiment can therefore yield the full information about the quantum state of the motion.

The Konstanz experiment is sketched in figure 2a. A discharge source for metastable helium atoms fires for 10 μs, generating a double-peaked distribution of atomic velocities consisting of slow atoms between about 1000 and 3000 m/s and fast atoms near 33 000 m/s. The corresponding de Broglie wavelengths are concentrated near 3 picometers for the fast atoms and between 20 and 70 pm for the slow atoms. A 5 μm wide entrance slit collimates this beam. Farther downstream, the beam passes through a microfabricated double-slit structure with a slit separation of 8 μm and openings of 1 μm. The combination of entrance slit and double slit acts as a preparation tool for the transverse motional quantum state of the atoms. After emerging from this preparation tool, the atoms propagate over a distance d to a time- and space-resolving detector. When each metastable atom strikes the detector, it releases a large amount of energy, allowing nearly every atom to be detected. The spatial and temporal coordinates of each such event at the detector are recorded. This data provides a measurement of spatial atomic distributions for different longitudinal velocities v in the beam, or equivalently, different propagation times $t_d = d/v$ from the double slit to the detector.

As discussed above, different propagation times t_d lead to different views of the Wigner distribution. Another way to look at this situation is to treat the atomic wavepacket evolution as an optical diffraction problem, in which the shear of the Wigner distribution corresponds to the transition from the Fresnel (near-field) regime to the Fraunhofer (far-field) regime. Figure 2c shows the results predicted by theory for atoms with a wide range of propagation times. In the extreme Fresnel regime, we recognize the spacelike shadow of the two slits. With increasing t_d, the wavepackets start to overlap and interfere until, for large t_d, we arrive at the Fraunhofer regime in which the diffraction pattern embodies the momentum-like shadow of the state. In figure 2, experimental measurements of the time-resolved diffraction patterns are shown on both sides of the theoretical plot. On the left, figure 2b corresponds to a distance $d = 195$ cm, the Fraunhofer regime for slow atoms. It shows nicely a resolved interference pattern that corresponds to the momentum-like shadow. The very fast atoms produce the spacelike shadow of the double slit at the bottom of figure. This measurement corresponds to two separate ranges of propagation times, or view angles, of the quantum state's Wigner distribution. The other view angles are missing because their respective atom velocities are absent from the atomic beam. To fill in these views, a second experiment is performed with the detector screen placed only $d = 25$ cm behind the double slit. Figure 2d shows the result of this experiment, which features the transition between the spreading individual wavepackets and the overlapping and interference of the slow atoms, in addition to the usual spacelike shadow of the very fast atoms at the bottom.

Figure 3 displays the Wigner distribution that is reconstructed by binning the data according to the different propagation times t_d and performing the inverse Radon transformation. Figure 3a shows the Wigner distribution reconstructed from the $d = 25$ cm data, and figure 3b shows the Wigner distribution derived from the $d = 195$ cm data. In both cases, we recognize two positive ridges corresponding to the spatial distribution of the atoms

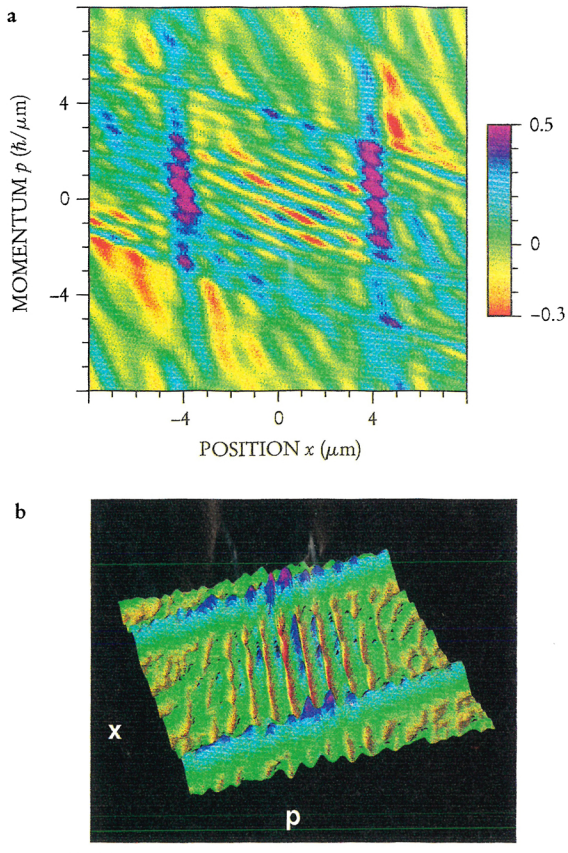

FIGURE 3: RECONSTRUCTED WIGNER DISTRIBUTIONS derived from the experimental data sets shown in figure 2d (corresponding to $d = 25$ cm) (**a**) and figure 2b ($d = 195$ cm) (**b**). Both reconstructions show the expected two lobes separated by the slit separation of 8 μm. Between the lobes, the Wigner distribution oscillates between positive and negative values, indicating the spatial coherence and nonclassical character of the state immediately behind the double slit.

immediately behind the double slit. These ridges are separated by 8 μm—the spacing of the double slit. The coherence between the two spatially separated parts of the wavefunction at the double slit leads to interference, reflected by the oscillations in the Wigner distribution in the region between the ridges. In this region, the reconstructed Wigner distribution assumes negative values, indicating a property that cannot be obtained by classical phase-space distributions and revealing the quantum nature of the observed ensemble of atoms. The reconstructed Wigner distributions, determined from about 500 000 atoms, exhibit all the features of a superposition state expected from an atom interferometer. The measured Wigner distributions differ in some respects from what is theoretically expected, including residual shear and spurious negative regions close to the two large positive ridges. These artifacts occur primarily because the reconstructions are from an incomplete range of projection angles.

Quantum mirrors and a trapped atom

To reconstruct the quantum state of motion of a single harmonically trapped atom, we turn to a more direct method that does not require the transformations involved in the tomographic technique described above. Instead,

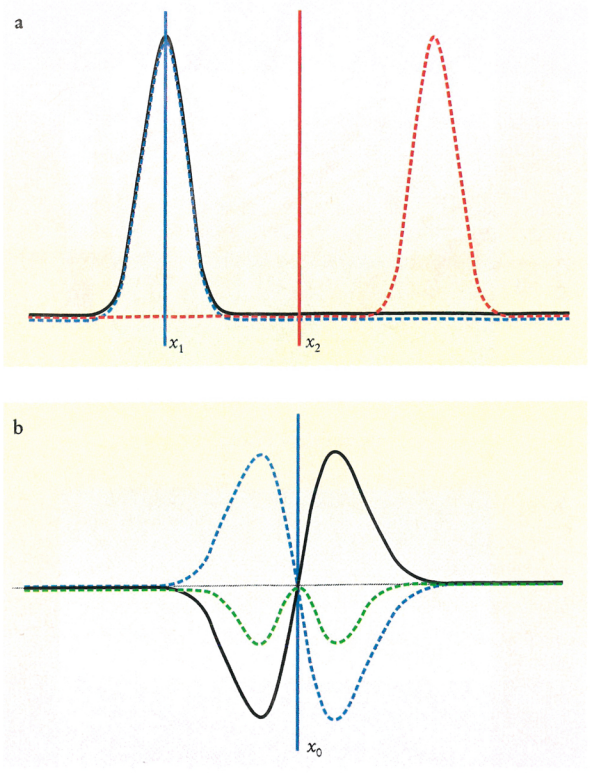

FIGURE 4: THE QUANTUM MIRROR. **a**: The classical-like case of a localized particle. If the initial wavefunction (solid black line) is mirrored around x_1, where the particle is localized, the mirror image (blue dashed line) lies right on top of the original and the overlap is large. If the mirror is at x_2, the image (red dashed line) has essentially no overlap with the original. Thus, the overlap is localized like the particle's probability distribution. **b**: The quantumlike case of a particle with coherent amplitudes in different locations. The wavefunction of the first excited ($n = 1$) energy eigenstate of a harmonic oscillator has a valley and a peak left and right of the origin (solid black line) and exhibits odd parity. Peak and valley are interchanged on the mirror image around $x_0 = 0$ (blue dashed line) and the overlap product of the two functions (dashed green line) is zero or negative everywhere. The value of the Wigner distribution at the origin of phase space is the area of the green curve, and is thus maximally negative for the $n = 1$ state.

the Wigner distribution at a particular point in phase space is extracted directly by performing several different measurements on an identically prepared system. This method is based upon a simple and powerful picture of the Wigner distribution that was first pointed out in 1977 by Antoine Royer.[8]

Suppose we create a mirror image of the wavefunction $\Psi_x(x)$ about the point x_0 and then measure the overlap of the mirror image $\mathcal{M}(x_0)\Psi_x(x) = \Psi_x(2x_0 - x)$ with the original $\Psi_x(x)$. Formally, this is a measurement of the expectation value m of the mirror operation $\mathcal{M}$,

$$m(x_0) = \langle\Psi_x|\mathcal{M}(x_0)|\Psi_x\rangle$$

$$= \frac{1}{2}\int ds\ \Psi_x^*\left(x_0 + \frac{s}{2}\right)\Psi_x\left(x_0 - \frac{s}{2}\right). \qquad (3)$$

If $\Psi_x(x)$ is localized around x_1, the mirror operation about $x_0 = x_1$ will largely map this area onto itself, resulting in a nonzero overlap. But if we perform the mirror operation about some other point x_2—far from x_1—the overlap with the original wavefunction will nearly vanish. (See figure 4a.) Thus, we might expect that the observed overlap $m(x_0)$ will be nonzero only for positions x_0 where $\Psi_x(x)$ is localized. But now suppose that the wavefunction is localized in two separated regions, centered at $-\tilde{x}$ and $\tilde{x}$. If we perform the mirror operation halfway in between, at $x_0 = 0$, the lobes of the mirrored wavefunction will nearly coincide with the original lobes, resulting in a large overlap. Moreover, the overlap will contain information about the phase difference between the original and mirrored wavefunction. For instance, in figure 4b, the two pieces of the wavefunction are 180° out of phase (a mountain and a valley), resulting in a negative value of the overlap between the wavefunction and its image.

Returning to equation 3, we note that the mirror expectation $m(x_0)$ is proportional to the Wigner distribution at zero momentum $W(x_0, 0)$. If the mirror operation could be performed about the phase-space coordinates (x_0, p_0), we might hope the Wigner distribution $W(x_0, p_0)$ could be extracted directly from a measurement of this modified overlap. Royer made this connection and saw that the mirror operator about the origin of phase space is just the parity operator Π. Therefore the Wigner distribution at (x_0, p_0) can be interpreted as the expectation of the displaced parity operator,

$$W(x_0, p_0) = \frac{1}{\pi}\langle\Psi|\mathcal{D}^\dagger(-x_0, -p_0)\,\Pi\,\mathcal{D}(-x_0, -p_0)|\Psi\rangle\,, \qquad (4)$$

where $\mathcal{D}(x, p)$ is the coherent displacement operator, which displaces a state across phase space by an amount (x, p) or, equivalently, shifts the origin of phase space from $(0, 0)$ to $(-x, -p)$.[9] The examples of figure 4 illustrate the connection between the overlap of wavefunction mirrors and the Wigner distribution, and figure 4b highlights a particular case in which the Wigner distribution can take on its peculiar negative values. These negative values occur only when the wavefunction is nonlocally distributed, thereby highlighting the nonclassical or delocalized features of the quantum state.

In experiments conducted by David Wineland's group at the National Institute of Standards and Technology in Boulder, Colorado,[10] a single $^9Be^+$ ion is confined in a radio frequency (Paul) ion trap. The trapping potential is well characterized by a three-dimensional anisotropic harmonic oscillator. We describe the measurement of the Wigner distribution for motion in one of the dimensions, characterized by the ladder of energy eigenstates $|n\rangle$ of energy $(n + \frac{1}{2})\hbar\omega$, where $n = 0, 1, 2, \ldots$, and $\omega/2\pi \approx 11$ MHz is the harmonic oscillation frequency. To reconstruct $W(x_0, p_0)$ in this system, the same quantum state must be prepared over and over. First, the ion is initialized in the harmonic oscillator ground state by laser cooling. (See the article by Wineland and Wayne Itano in PHYSICS TODAY, June 1987, page 34.) Next, a particular motional state is prepared in a controlled fashion by applying laser pulses and RF fields. A variety of harmonic oscillator states can be created, including thermal, coherent, squeezed and energy eigenstates (number states),[11] and superpositions of these types of states, including "Schrödinger's cat" states.[12] The relative phases of these states of motion can be controlled by the stable relative phases of the laser and RF fields used in their creation.

The quantum mirror measurement of the Wigner distribution requires two ingredients: a coherent displacement of the state (equivalent to a displacement of the phase-space origin), and a way to determine the expectation value of the parity operator of this displaced state.

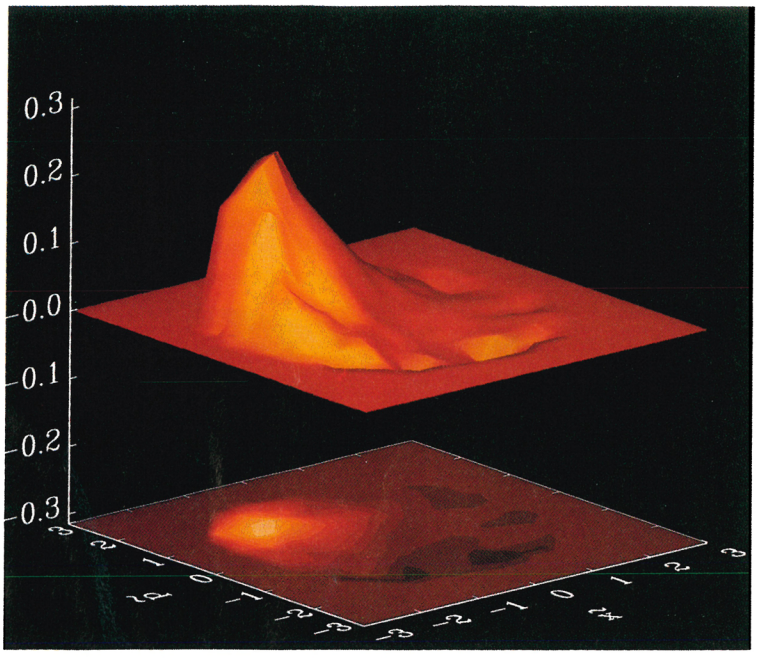

FIGURE 5: A CLASSICAL-LIKE COHERENT STATE of a harmonic oscillator (in this case an ion of mass m in a trap) produces this experimentally reconstructed Wigner distribution. The ion's coordinates of position x and momentum p are scaled to $x' = x\sqrt{m\omega/\hbar}$ and $p' = p/\sqrt{m\hbar\omega}$ and further transformed to a frame $(\tilde{x}, \tilde{p})$ that rotates at the harmonic trap frequency ω, in which the Wigner distribution is stationary. The center of gravity is about 2 scaled units from the origin, and the roughly circular Gaussian shape has nearly the minimum uncertainty width allowed by the Heisenberg uncertainty relationship ($\Delta\tilde{x}\Delta\tilde{p} \approx \frac{1}{2}$).

The displacement operator is achieved by applying an oscillating (resonant) electric field, which couples to the ion's harmonic motion, similar to pushing (or stopping) a child on a swing. In principle, the state can be coherently displaced by any amount (x_0, p_0) in phase space by varying the amplitude of the applied field and its phase with respect to that of the initial state of motion. The expectation value of the parity operator after the displacement can be determined by measuring the populations of energy eigenstates, which, for a harmonic oscillator, are also parity eigenstates. That is, states $|n\rangle$ with an even or odd number of energy quanta n have even or odd parity, respectively. Therefore, the expectation of the parity operator can be deduced by simply measuring the probability distribution $P_n(x_0, p_0)$ of energy eigenstates of the displaced state and performing an alternating sum over these probabilities. Substituting this result in equation 4, we find that the Wigner distribution is

$$W(x_0, p_0) = \frac{1}{\pi} \sum_{n=0}^{\infty} (-1)^n P_n(x_0, p_0) . \qquad (5)$$

The measurement of the motional state occupation probabilities $P_n(x_0, p_0)$ is tricky, because it is very difficult to detect a single ion's motion directly. Instead, features of the motional state are encoded onto two internal electronic (hyperfine) levels of the ion, labeled $|\downarrow\rangle$ and $|\uparrow\rangle$. The occupation of these states can be detected with nearly 100% quantum efficiency by applying laser radiation that connects one of the hyperfine levels (say $|\downarrow\rangle$) to an excited electronic state. If the ion is in state $|\downarrow\rangle$, it scatters thousands of photons, an event that can easily be detected. If, on the other hand, the ion is in state $|\uparrow\rangle$, essentially no photons will be scattered.[13] To encode the motional states onto the internal states of the ion, a "mapping interaction" is realized with laser beams. For an appropriate tuning of the lasers, the external motion is coupled to the internal hyperfine levels, and energy is periodically exchanged between the two systems, similarly to energy exchange between two coupled pendulums. The exchange frequency (or Rabi frequency) Ω_n between $|\downarrow\rangle$ and $|\uparrow\rangle$ due to this mapping interaction is different for each motional eigenstate $|n\rangle$, and if the atom is initially in state $|\downarrow\rangle$, after the mapping interaction is applied for a time τ, its probability of being in state $|\downarrow\rangle$ is[11]

$$P_{\downarrow}(\tau) = \sum_{n=0}^{\infty} P_n(x_0, p_0) \cos^2(\Omega_n \tau) . \qquad (6)$$

This whole process—initial state preparation, displacement by (x_0, p_0), mapping interaction for time τ, measurement of $P_{\downarrow}(\tau)$—is repeated for different values of interaction time τ. The motional probabilities $P_n(x_0, p_0)$ are then extracted from equation 6 by Fourier transforming the measured $P_{\downarrow}(\tau)$ at the known frequencies Ω_n.

Figure 5 shows the reconstructed Wigner distribution for the single trapped ion in a classical-like coherent state, which is simply a wavepacket oscillating in the harmonic potential without changing shape. In the laboratory frame, the Wigner distribution rotates in phase space at the harmonic trap frequency ω, but here the reconstruction is performed in the rotating frame (rotating in phase space), where $W(x, p)$ is stationary. Within the limits of experimental uncertainty, the reconstructed Wigner distribution is positive everywhere and the nearly Gaussian hump has a width close to the Heisenberg limit, which is $\Delta\tilde{x}\,\Delta\tilde{p} \approx \frac{1}{2}$ in the scaled coordinates (this is most obvious in the contour plot at the bottom of the figure).

Figure 6 shows the reconstructed Wigner distribution of the first excited energy eigenstate of the harmonic oscillator (that is, the $n = 1$ Fock state). Although Fock states of the harmonic oscillator are treated in every introductory quantum mechanics textbook, the NIST experiments represent the first time Fock states (other than the $n = 0$ ground state) have been created on demand and fully characterized. (In many quantum optics experiments, single-photon states have been produced using down-conversion, but such states are not created on demand—they occur at random moments in a nonlinear crystal—and their mode identity is not well defined.) In accord with the nonclassical nature of this state, the Wigner distribution is negative around the origin. The experimental reconstruction in the figure reaches approximately −0.25 at the origin of phase space, not far from the theoretical value of $-1/\pi$, which is in fact the largest negative value the Wigner distribution (as defined in

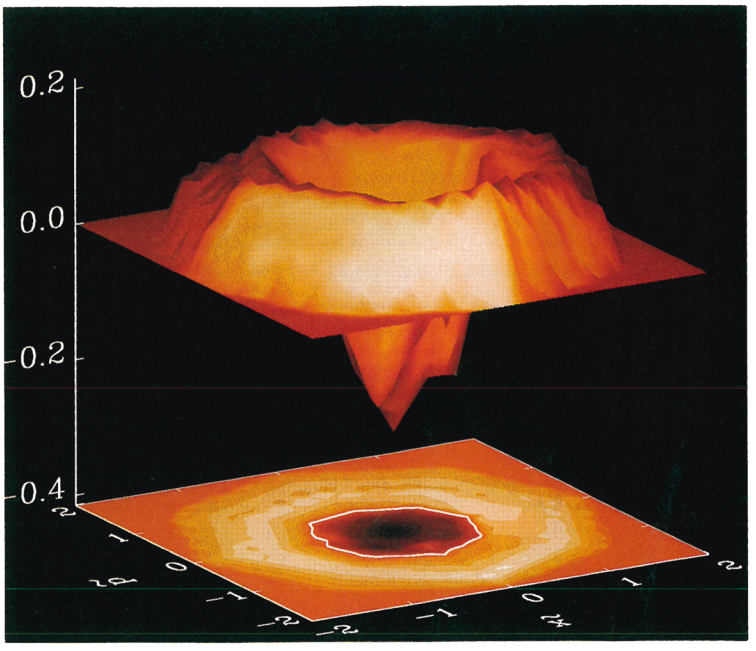

FIGURE 6: THE FIRST EXCITED ENERGY eigenstate of a harmonic oscillator produces this experimentally reconstructed Wigner distribution. The coordinates $\tilde{x}$ and $\tilde{p}$ are scaled and in a rotating frame, as in figure 5. Because energy and phase are complementary, the measured function is nearly rotationally symmetric, providing no phase information. The measured values of the Wigner distribution near the origin are negative and reach a minimum value of about −0.25 at the origin. This is close to the largest negative value possible ($-1/\pi$) for a Wigner distribution.

equation 1) can reach in any physical system. Discrepancies with respect to theory can be traced to slight imperfections in the preparation and are not surprising, considering the stability required of the experimental parameters—the reconstructions are the result of about 24 million preparations of the same state. Nevertheless, the reconstructed Wigner distributions correspond very closely to that of a pure quantum state.

Applications for quantum trickery

The Wigner distribution $W(x, p)$ corresponds most closely to the idea of a phase-space probability distribution in quantum mechanics, making it a useful tool for characterizing quantum states. We've seen that the Wigner distribution is not a real probability distribution, because certain joint events (such as simultaneous position and momentum states) are inaccessible. Localized negative values of $W(x, p)$ emphasize this fact. To make a connection between the quantum Wigner distribution and the "negative probabilities" derived in table 3 for flipping coins in a black box, we're tempted to identify the joker in the black box as Heisenberg himself, who somehow knows what is to be measured each time, and changes the results of the coin tosses accordingly. And yet, in a sense, quantum mechanics is stranger still than this picture, for the wavefunction or the Wigner distribution ensures the consistency of different measurements without any need for such a trickster behind the scenes.

The recent experiments we have discussed, in which quantum states of matter waves have been reconstructed by mapping their Wigner distributions, were made possible by advances in quantum state preparation and manipulation. These newly developed measurement techniques have abundant future applications. For instance, in the fields of quantum control and quantum computing, these techniques could be extended to provide a complete picture of the evolution of a quantum logic gate. Control and diagnostics of an atomic beam at the quantum level might be a helpful tool in deposition techniques reaching quantum-limited resolution. An intriguing prospect would be to reconstruct the output state of laserlike sources of atoms that might evolve from the current research in Bose–Einstein condensates of dilute gases. A fundamental application of these techniques will be the study of quantum decoherence. The reconstruction of a quantum state as it loses coherence may someday shed light on the elusive mechanisms at work when a wavefunction "collapses."

We thank our coworkers David Wineland, Wayne Itano, Dawn Meekhof and Brian King at NIST; and Christian Kurtsiefer, Martin Wilkens, Ulf Janicke and Jürgen Mlynek at the University of Konstanz. We give special thanks to Ben Stein of the American Institute of Physics for suggesting this article and Matt Young at NIST for carefully reading the manuscript. The work at NIST was supported by the National Security Agency, the Army Research Office and the Office of Naval Research. One of us (Leibfried) acknowledges a German Research Foundation (DFG) research grant. The work at the University of Konstanz was supported by the DFG.

References

1. This example was inspired by an article by R. P. Feynman, "Negative Probabilities," in *Quantum Implications: Essays in Honor of David Bohm*, B. J. Hiley, F. D. Peat, eds., Routledge & Kegan Paul, London (1987), p. 235. See also R. P. Feynman, Int. J. Theor. Phys. **21**, 467 (1982).
2. E. P. Wigner, Phys. Rev. **40**, 749 (1932).
3. For general references on this subject, see Ulf Leonhardt, *Measuring the Quantum State of Light*, Cambridge U. P., New York (1997). M. G. Raymer, Contemp. Physics **38**, 343 (1997). W. P. Schleich, M. G. Raymer, eds., special issue of J. Mod. Opt., **44**, no. 11/12 (1997).
4. D. T. Smithey, M. Beck, M. G. Raymer, A. Faridani, Phys. Rev. Lett. **70**, 1244 (1993).
5. T. J. Dunn, I. A. Walmsley, S. Mukamel, Phys. Rev. Lett. **74**, 884 (1995).
6. M. G. Raymer, M. Beck, D. F. McAlister, Phys. Rev. Lett. **72**, 1137 (1994). U. Janicke, M. Wilkens, J. Mod. Opt. **42**, 2183 (1995).
7. C. Kurtsiefer, T. Pfau, J. Mlynek, Nature **386**, 150 (1997).
8. A. Royer, Phys. Rev. A **15**, 449 (1977).
9. R. J. Glauber, Phys. Rev. **131**, 2766 (1963).
10. D. Leibfried, D. M. Meekhof, B. E. King, C. Monroe, W. M. Itano, D. J. Wineland, Phys. Rev. Lett. **77**, 4281 (1996).
11. D. M. Meekhof, C. Monroe, B. E. King, W. M. Itano, D. J. Wineland, Phys. Rev. Lett. **76**, 1796 (1996).
12. C. Monroe, D. M. Meekhof, B. E. King, D. J. Wineland, Science **272**, 1131 (1996).
13. R. Blatt, P. Zoller, Eur. J. Phys. **9**, 250 (1988). ■